


Engineering Applications of Computational Fluid Mechanics >  
Volume 13, 2019 - Issue 1 Open access

2,140 Views | 35 CrossRef citations to date | 0 Altmetric


Listen

Articles

# Applicability of connectionist methods to predict dynamic viscosity of silver/water nanofluid by using ANN-MLP, MARS and MPR algorithms

Mohammad Hossein Ahmadi , Behnam Mohseni-Gharyehsafa, Mahmood Farzaneh-Gord, Ravindra D. Jilte, Ravinder Kumar & Kwok-wing Chau

Pages 220-228 | Received 02 Dec 2018, Accepted 15 Jan 2019, Published online: 05 Mar 2019

 Cite this article  <https://doi.org/10.1080/19942060.2019.1571442> Check for updates Full Article Figures & data References Citations Metrics Licensing Reprints & Permissions View PDF View EPUB

## ABSTRACT

Formulae display:  MathJax 

Dynamic viscosity considerably affects the heat transfer and flow of fluids. Due to improved thermophysical properties of fluids containing nanostructures, these types of fluids are widely employed in thermal mediums. The nanofluid's dynamic viscosity

### About Cookies On This Site

We and our partners use cookies to enhance your website experience, learn how our site is used, offer personalised features, measure the effectiveness of our services, and tailor content and ads to your interests while you navigate on the web or interact with us across devices. You can choose to accept all of these cookies or only essential cookies. To learn more or manage your preferences, click "Settings". For further information about the data we collect from you, please see our [Privacy Policy](#).

Accept All

Essential Only

Settings



models are 0.9998, 0.9997 and 0.9996 for the ANN-MLP, MARS and MPR algorithms, respectively. In addition, based on importance analysis, the temperature is highly effective and the dominant parameter for the dynamic viscosity of the nanofluid in comparison with size and concentration.

Q KEYWORDS: nanofluid dynamic viscosity artificial neural network concentration multivariate adaptive regression splines (MARS) multivariable polynomial regression (MPR)

## Nomenclature

$\varphi$	=	Concentration
T	=	Temperature (°C)
d	=	Size (nm)
$\mu$	=	Dynamic viscosity
$a_i$	=	Coefficients in MPR method
$b_i$	=	Coefficients in MARS method

BF

GC

AAPRE



### About Cookies On This Site

We and our partners use cookies to enhance your website experience, learn how our site is used, offer personalised features, measure the effectiveness of our services, and tailor content and ads to your interests while you navigate on the web or interact with us across devices. You can choose to accept all of these cookies or only essential cookies. To learn more or manage your preferences, click “Settings”. For further information about the data we collect from you, please see our [Privacy Policy](#).

- Accept All
- Essential Only
- Settings



RMSE	=	Root mean square error
R2	=	Coefficient of determination
MARS	=	Multivariate adaptive regression splines
MPR	=	Multivariable polynomial regression
ANN	=	Artificial neural network
MLP	=	Multilayer perceptron
C(M)	=	Complexity penalty

## 1. Introduction

Nano-sized materials such as nanosheets or nanoparticles can be dispersed in a base fluid to prepare nanofluids (Ahmadi, Mirlohi, Nazari, & Ghasempour, [2018](#); Nazari, Ghasempour, Ahmadi, Heydarian, & Shafii, [2018](#)). According to the literature, nanofluids, due to adjustable properties and high stable dispersion, may be used in various applications such as heat exchangers, solar collectors, and cooling systems. Moreover, nanofluids can be used in various industrial systems to enhance the efficiency of the process. For example, Wang & Jiao, [2015](#), and Wang & Jiao, [2015](#), studied the effect of nanofluids on the heat transfer coefficient. Adding nanofluids to the base fluid can increase the heat transfer coefficient, etc.

### About Cookies On This Site

We and our partners use cookies to enhance your website experience, learn how our site is used, offer personalised features, measure the effectiveness of our services, and tailor content and ads to your interests while you navigate on the web or interact with us across devices. You can choose to accept all of these cookies or only essential cookies. To learn more or manage your preferences, click "Settings". For further information about the data we collect from you, please see our [Privacy Policy](#).

Accept All

Essential Only

Settings





temperature, synthesis procedure, pH and concentration is investigated in several pieces of research (Baghban, Jalali, Shafiee, Ahmadi, & Chau, [2019](#); Hosseini, Kasaeian, Pourfayaz, Sheikhpour, & Wen, [2018](#); Zeinali Heris, Kazemi-Beydokhti, Noie, & Rezvan, [2012](#)).

The dynamic viscosity of nanofluids significantly affects their fluid flow and heat transfer (Ahmadi et al., [2018](#); Ebrahimi-Moghadam, Mohseni-Gharyehsafa, & Farzaneh-Gord, [2018](#); Mohseni-Gharyehsafa et al., [2018](#); Nazari, Ahmadi, Ghasempour, & Shafii, [2018](#)). Given this fact, it is critical to get better awareness of the parameters affecting this property. According to the literature review, an increase in temperature results in lower dynamic viscosity, which facilitates fluid motion due to the reduction in friction. Another effective factor in dynamic viscosity is the concentration of nanostructures dispersed in the base fluid (Chiam, Azmi, Usri, Mamat, & Adam, [2017](#); Soltani & Akbari, [2016](#)). On the basis of the results of experimental studies, an increase in concentration leads to an improvement of dynamic viscosity (Asadi & Asadi, [2016](#)). The size of nanostructures plays a key role in thermophysical properties of nanofluids.

Artificial neural networks are widely employed for modeling the system and pattern recognition. Artificial neural networks are applicable in modeling the thermophysical properties of nanofluids (Ahmadi, Tatar, Nazari, Mahian, & Ghasempour, [2018](#); Chau, [2017](#); Kazemi et al., [2018](#); Rezaei, Sadeghzadeh, Alhuyi Nazari, Ahmadi, & Astaraei, [2018](#)). Ahmadi et al. ([2018](#)) employed the least square support vector machine (LSSVM) and group method of data handling (GMDH) approaches to model the thermal conductivity value of CuO/EG (Copper-Oxide/Ethylene-Glycol) nanofluid. It was monitored from the outcomes that the  $R^2$  values for GMDH and LSSVM were equal to 0.994 and 0.991, respectively. These values indicated the high accuracy of the models in estimating the nanofluid's thermal conductivity. In another piece of research (Ahmadi et al., [2018](#)), LSSVM was employed to predict the thermal conductivity of alumina/EG.

The  $R^2$  v Baghban et al. ([2018](#)) coefficients of the con dependent param Statistical crite highest accuracy To propo ng the

#### About Cookies On This Site

We and our partners use cookies to enhance your website experience, learn how our site is used, offer personalised features, measure the effectiveness of our services, and tailor content and ads to your interests while you navigate on the web or interact with us across devices. You can choose to accept all of these cookies or only essential cookies. To learn more or manage your preferences, click "Settings". For further information about the data we collect from you, please see our [Privacy Policy](#).

Accept All

Essential Only

Settings





concentration when modeling thermophysical properties; adding size as another input variable results in more accurate results. In the current study, the Ag/water nanofluid's dynamic viscosity is modeled by applying MPR, ANN-MLP and MARS algorithms. The input variables in the modeling process are temperature, size and volumetric concentration.

## 2. Intelligent modes

### 2.1. Multilayer perceptron neural network

Artificial neural networks are conventionally applied for prediction purposes. MLP is a feed-forward neural network algorithm. This network is composed of an input layer, hidden layer and output layer (Gardner & Dorling, [1998](#); Hornik, Stinchcombe, & White, [1989](#)). The number of input and output layers depends on the data. In the hidden layer, one or more layers can exist that have various neurons (Orhan, Hekim, & Ozer, [2011](#)). In these types of neural networks, the initial neuron of the layer is fed into the neuron of layer in the next stage, which is the same for all layers except the first layer. Each neuron has an activation function and a sum function. The inputs are initially multiplied by the weighting factor and added to each other. Afterwards, a bias factor is added to the calculated number. In the next step, the number obtained from the summing function is used in the activation function as input data. Activation functions are categorized in three forms as represented below, where  $\phi$  is the activation function (Ruck, Rogers, Kabrisky, Oxley, & Suter, [1990](#); Vanzella et al., [2004](#)).

$\phi(r) = \exp(-r^2/2\sigma^2)$  (1) In the above equation,  $\sigma > 0$  is the width, which shows the interpolating function smoothness. The distance between  $x$  and the center is defined by  $r$ .

#### About Cookies On This Site

We and our partners use cookies to enhance your website experience, learn how our site is used, offer personalised features, measure the effectiveness of our services, and tailor content and ads to your interests while you navigate on the web or interact with us across devices. You can choose to accept all of these cookies or only essential cookies. To learn more or manage your preferences, click "Settings". For further information about the data we collect from you, please see our [Privacy Policy](#).

Accept All

Essential Only

Settings





MARS is applied in regression and data classification (Friedman & Roosen, [1995](#)). This approach is mainly utilized to predict the dependent data,  $Y$  ( $n \times 1$ ), which are continuous, based on the group of input data ( $n \times p$ ). This model is represented as follows:

$$y = f(x) + e \quad (2)$$

In the above equation,  $f$  indicates the weighted sum of basic functions. These functions are dependent on  $X$ . In addition,  $e$  stands for the error, which is an ( $n \times 1$ ) matrix. In this method, no priori assumption is required for estimating the relationship between dependent and independent data. The relationship between these data is found on the basis of a group of coefficients and piecewise polynomials. The model is generated using this algorithm based on fitting basic functions to independent variables' distinct intervals. Typically, the polynomials that are called "splines" consist of pieces connecting to each other. The connecting points of the splines are known as "nodes," "knots" or "breakdown points." The points are shown by  $t$ . In a  $q$ -degree spline, each section is a polynomial function. The function utilized by the MARS algorithm is described as:

$$[-(x-t)]_+^q = (t-x)^q \text{ if } x < t \quad 0 \text{ otherwise} \quad (3)$$

$$[+(x-t)]_+^q = (x-t)^q \text{ if } x \geq t \quad 0 \text{ otherwise} \quad (4)$$

In the above equation,  $q$  ( $\geq 0$ ) is the power at which the splines are boosted up. The smoothness of the obtained function depends on the value of  $q$ . In the case of  $q = 1$ , as in the present study, just simple linear splines are applied. In Figure 1, a pair of splines for the node  $t = 3.5$  is shown.

Figure 1. Spline at  $t = 3.5$  (Nieto, García-Gonzalo, Bernardo Sanchez, & Menendez Fernandez, [2016](#)).



### About Cookies On This Site

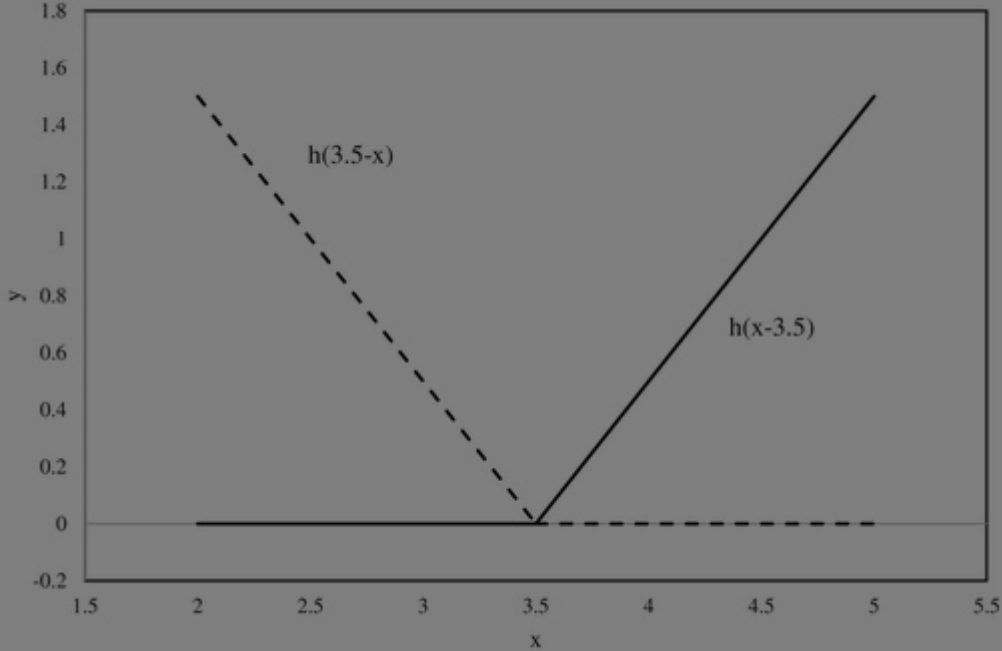
We and our partners use cookies to enhance your website experience, learn how our site is used, offer personalised features, measure the effectiveness of our services, and tailor content and ads to your interests while you navigate on the web or interact with us across devices. You can choose to accept all of these cookies or only essential cookies. To learn more or manage your preferences, click "Settings". For further information about the data we collect from you, please see our [Privacy Policy](#).

Accept All

Essential Only

Settings





Display full size

By considering  $y$  which has  $M$  bias functions, the model proposed by MARS can be written (Chou, Lee, Shao, & Chen, [2004](#); De Cos Juez, Lasheras, García Nieto, & Suárez, [2009](#); Friedman & Roosen, [1995](#); Nieto & Antón, [2014](#); Nieto, Fernández, Lasheras, de Cos Juez, & Muñiz, [2012](#); Nieto, Lasheras, de Cos Juez, & Fernández, [2011](#); Orhan et al., [2011](#); Xu et al., [2004](#)) as:

$$\hat{y} = f^M(x) = c_0 + \sum_{m=1}^M c_m B_m(x) \quad (5)$$

$\hat{y}$  indicates the parameter predicted by MARS,  $c_0$  is a fixed value, the  $m$ th bias function is referred to as  $B_m(x)$  and  $c_m$  refers to the  $m$ th basic function's coefficient. It is crucial to optimize the variables ( $c_0$  and  $c_m$ )

announced into the knot positions and the model. For a dataset of  $X$  which has  $n$  objects and  $p$  input variables,  $N = n \times p$  pairs of spline basic functions exist which can be calculated using Equations (3) and (4). In order to generate the final model, a two-step process must be followed. In the first stage, a two-at-a-time forward stepwise process is performed to choose the basic functions (Chou et al., [2004](#); De Cos Juez et al., [2009](#); Friedman & Roosen, [1995](#); Nieto & Antón, [2014](#); Nieto et al., [2012](#); Nieto et al., [2011](#);

Orhan et al., [2011](#); Xu et al., [2004](#)) as:

with inap

the mod

removed

func

Roosen,

al., [2004](#)

divided

### About Cookies On This Site

We and our partners use cookies to enhance your website experience, learn how our site is used, offer personalised features, measure the effectiveness of our services, and tailor content and ads to your interests while you navigate on the web or interact with us across devices. You can choose to accept all of these cookies or only essential cookies. To learn more or manage your preferences, click "Settings". For further information about the data we collect from you, please see our [Privacy Policy](#).

to a model

erfitting of

ay be

usable

man &

[2011](#); Xu et

dual error

culated as



$$GCV(M) = \frac{1}{n} \sum_{i=1}^n (y_i - \hat{f}_M(x_i))^2 (1 - C(M)/n)^2 \quad (6)$$

$C(M)$  refers to complexity penalty, which depends on the number of basic functions and can be obtained (Chou et al., [2004](#); De Cos Juez et al., [2009](#); Friedman & Roosen, [1995](#); Nieto & Antón, [2014](#); Nieto et al., [2012](#), [2011](#); Orhan et al., [2011](#); Xu et al., [2004](#)) as:  $C(M) = (M+1) + dM$  (7)  $M$  refers to the number of functions used as basic in Equation (5);  $d$  indicates a penalty for the basic functions utilized in the proposed model. Increase in the value of  $d$  causes fewer required basic functions and smoother estimation.


When the MARS model is generated, the importance of the utilized variables for modeling can be assessed. Taking into account the literatures several criteria can be applied which in this study, the GCV parameter is used for this purpose to achieve reliable results (Chou et al., [2004](#); De Cos Juez et al., [2009](#); Friedman & Roosen, [1995](#); Nieto & Antón, [2014](#); Nieto et al., [2012](#), [2011](#); Orhan et al., [2011](#); Xu et al., [2004](#)).

### 3. Results and discussion

#### 3.1. Multivariable polynomial regression

In this study, experimental results from previous publications are used to model the range of the input variables and represented in Table 1. The data used for the modeling step are taken from experiments that were published recently (Alade, Oyehan, Popoola, Olatunji, & Bagudu, [2018](#); Esfe, Saedodin, Biglari, & Rostamian, [2016](#); Nikkam & Toprak, [2018](#)). The temperature of the fluid and the concentration ratio of the Ag/water nanofluid are those major elements which considerably affect the value of dynamic viscosity as illustrated in Figure 2.

Figure 2. Dynamic viscosity of Ag/water versus concentration and temperature.



#### About Cookies On This Site

We and our partners use cookies to enhance your website experience, learn how our site is used, offer personalised features, measure the effectiveness of our services, and tailor content and ads to your interests while you navigate on the web or interact with us across devices. You can choose to accept all of these cookies or only essential cookies. To learn more or manage your preferences, click "Settings". For further information about the data we collect from you, please see our [Privacy Policy](#).

Accept All

Essential Only

Settings



Table 1. Ranges of input variables (Alade et al., 2018 ; Esfe et al., 2016 ; Nikkam & Toprak, 2018 )



Download CSV

Display Table


By using 2D multivariate polynomial regression and applying the least square method (Royston & Sauerbrei, 2008; Sinha, 2013), a simple equation is obtained for the experimental data that is represented in Alade et al. (2018), Esfe et al. (2016) and Nikkam and Toprak (2018). The proposed model has three inputs including temperature, size of nanoparticles and volumetric concentration. This model is very simple, lacking any exponential or logarithmic term. The complex models obtained by neural networks have some disadvantages such as high computational cost. The coefficients of the model are shown in Equation (8):

$$\mu=a_1+a_2\times T+a_3\times\phi+a_4\times d+a_5\times T\times\phi+a_6\times d\times T+a_7\times d\times\phi+a_8\times\phi^2+a_9\times T^2 \quad (8)$$

3.2. Multivariate adaptive regression splines

As mentioned earlier, in the MARS algorithm, the cores of procedure are basic functions; therefore, it is necessary to choose appropriate ones. Unlimited increase in the basic functions causes overfitting. In this study, the sensitivity of the MARS model based on the input basic functions is investigated. According to Jerome H. Friedman (1991), the GCV method is used to obtain the optimal number of functions in which using 10 basic functions leads to the best results (Figure 3). The coefficients of the proposed model in Equation (8) are reported in Table 2.

Figure 3. GCV versus number of basic functions.



About Cookies On This Site

We and our partners use cookies to enhance your website experience, learn how our site is used, offer personalised features, measure the effectiveness of our services, and tailor content and ads to your interests while you navigate on the web or interact with us across devices. You can choose to accept all of these cookies or only essential cookies. To learn more or manage your preferences, click "Settings". For further information about the data we collect from you, please see our [Privacy Policy](#).

Accept All

Essential Only

Settings



Table 2. Coefficients of the proposed models

Display Table



The model obtained using 10 basic functions is represented in Equation (9). The coefficients of the proposed model in Equation (9) are reported in Table 2.

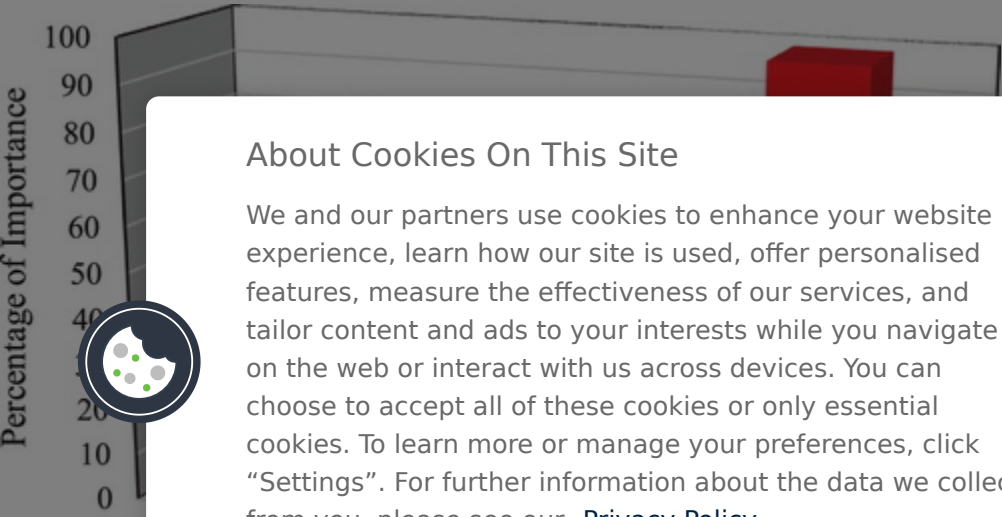
$$\mu = b_7 + b_8 \times BF_1 + b_9 \times BF_2 + b_{10} \times BF_3 + b_{11} \times BF_4 + b_{12} \times BF_5 + b_{13} \times BF_6 + b_{14} \times BF_7 + b_{15} \times BF_8 + b_{16} \times BF_9 + b_{17} \times BF_{10} \quad (9)$$

$$BF_1 = \text{Max}(0, T - b_1); BF_2 = \text{Max}(0, b_1 - T) BF_3 = \text{Max}(0, \phi - b_2); BF_4 = \text{Max}(0, b_2 - \phi) BF_5 = \text{Max}(0, b_3 - d); BF_6 = \text{Max}(0, b_4 - T) BF_7 = BF_5 \times \text{Max}(0, b_2 - \phi); BF_8 = BF_1 \times \text{Max}(0, \phi - b_5) BF_9 = BF_1 \times \text{Max}(0, b_5 - \phi); BF_{10} = BF_4 \times \text{Max}(0, b_6 - T)$$

In most of the studies in which the MARS method is used for regression modeling, the importance of data is calculated for gaining better insight into the influential parameters. Data whose importance is equal to 0 will be removed.

In order for gaining the relative importance of one parameter, the root square of the GCV of the all basis function without involving the propsed parameter should be obtain and then the value must be scaled to 100. Based on importance data analysis, temperature has the most significant effect compared with temperature and concentration (Figure 4). The concentration of nanofluid has the second rank in the calculation of dynamic viscosity.

Figure 4. Importance of input variables.



About Cookies On This Site

We and our partners use cookies to enhance your website experience, learn how our site is used, offer personalised features, measure the effectiveness of our services, and tailor content and ads to your interests while you navigate on the web or interact with us across devices. You can choose to accept all of these cookies or only essential cookies. To learn more or manage your preferences, click “Settings”. For further information about the data we collect from you, please see our [Privacy Policy](#).

Accept All

Essential Only

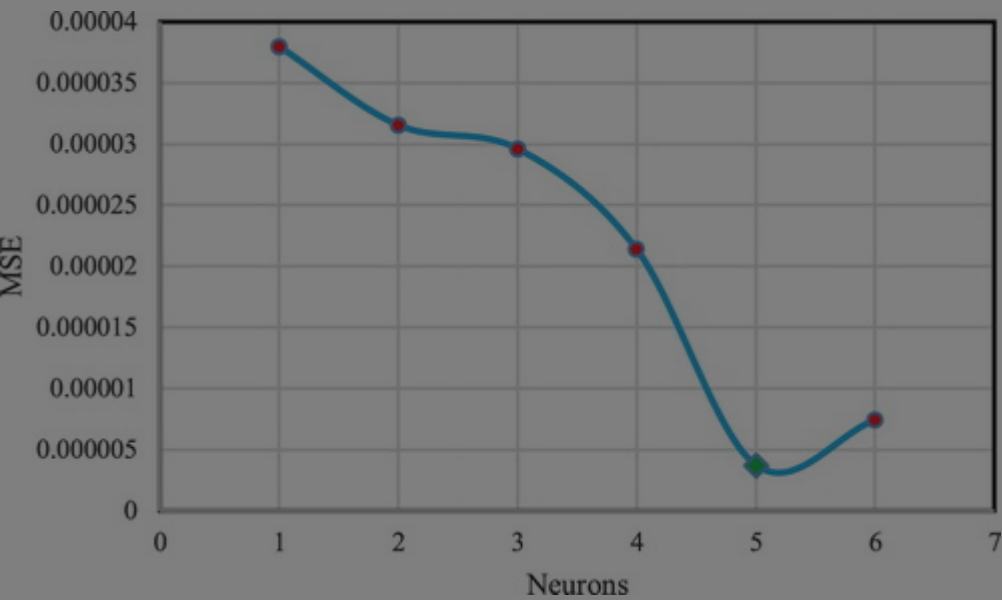
Settings



### 3.3. MLP-LMA: feed-forward back propagation with Levenberg-Marquardt training Algorithm

In MLP neural networks, hidden layers and their neurons play the key role in regression. Inappropriate model selection and an inadequate number of layers and neurons lead to unfavorable outputs. Therefore, it is necessary analyze the sensitivity of the network to the number of neurons and hidden layers. Since there are three input variables, a hidden layer is appropriate to obtain acceptable training; however, the sensitivity of the network must be considered based on the number of neurons. In the present study, MSE is used as criterion to select the optimum number of neurons. As shown in Figure 5 , using neurons leads to the best model.

Figure 5. MSE value for various number of neurons.



Neural Network identifier: 75% of data were used for training the network, 15% for validation

hidden l

best mo

7 are

conce

nanoflui

0.012 in

#### About Cookies On This Site

We and our partners use cookies to enhance your website experience, learn how our site is used, offer personalised features, measure the effectiveness of our services, and tailor content and ads to your interests while you navigate on the web or interact with us across devices. You can choose to accept all of these cookies or only essential cookies. To learn more or manage your preferences, click “Settings”. For further information about the data we collect from you, please see our [Privacy Policy](#).

Accept All

Essential Only

Settings

for the

layer. The

figures 6 and

on the

of Ag/water

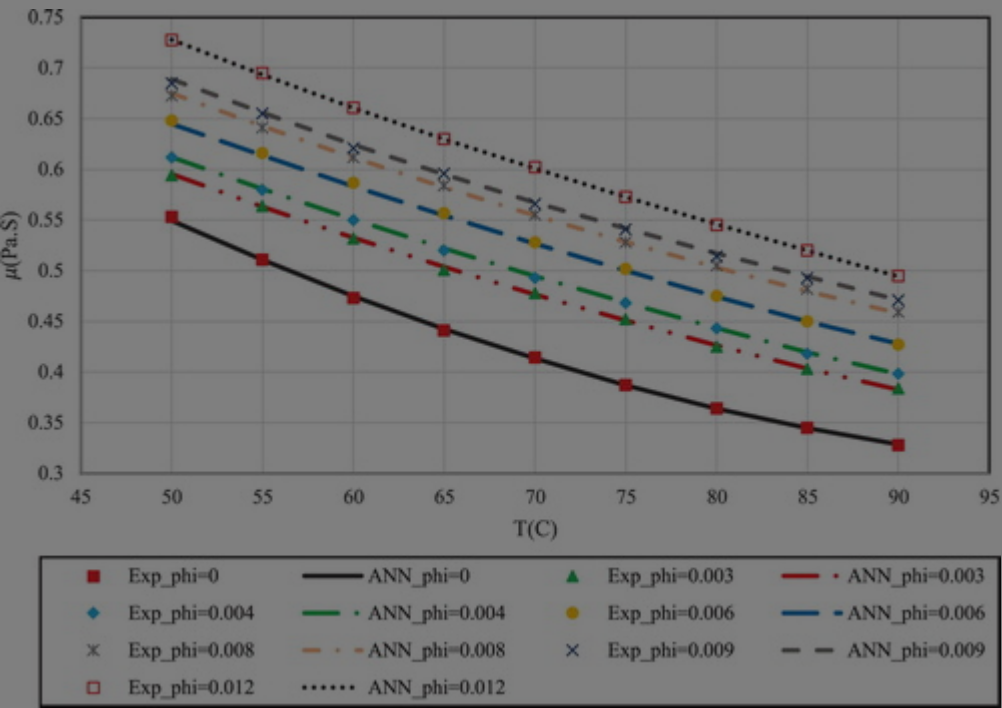
.009 and

les in these



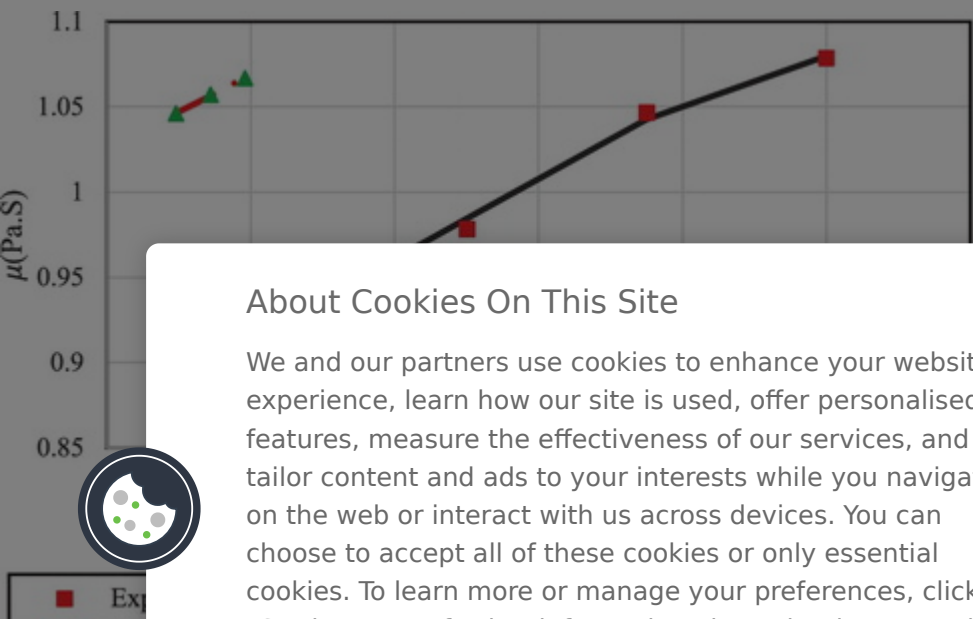
dynamic viscosity for each temperature. In addition, it can be concluded that higher temperature causes lower dynamic viscosity for a constant concentration. For instance, increasing the temperature from 50 to 70°C in 0.003 concentration leads to approximately 19.5% reduction in dynamic viscosity.

Figure 6 Dynamic viscosity of Ag/water nanofluid in different temperatures and concentrations.



Display full size

Figure 7. Dynamic viscosity of Ag/water nanofluid versus temperature and concentration.



About Cookies On This Site

We and our partners use cookies to enhance your website experience, learn how our site is used, offer personalised features, measure the effectiveness of our services, and tailor content and ads to your interests while you navigate on the web or interact with us across devices. You can choose to accept all of these cookies or only essential cookies. To learn more or manage your preferences, click “Settings”. For further information about the data we collect from you, please see our [Privacy Policy](#).

Accept All

Essential Only

Settings








into the influential factors. Based on the obtained values, the importance of temperature, concentration and size was approximately 100%, 80% and 12%, respectively. These values indicate the high importance of temperature in modeling the dynamic viscosity.

## Disclosure statement

No potential conflict of interest was reported by the authors.

## References

1. Ahmadi, M.-A., Ahmadi, M. H., Alavi, M. F., Nazemzadegan, M. R., Ghasempour, R., & Shamshirband, S. (2018). Determination of thermal conductivity ratio of CuO/ethylene glycol nanofluid by connectionist approach. *Journal of the Taiwan Institute of Chemical Engineers*, 91, 383–395.

 | [Web of Science ®](#) | [Google Scholar](#)

2. Ahmadi, M. H., Ahmadi, M. A., Nazari, M. A., Mahian, O., & Ghasempour, R. (2018). A proposed model to predict thermal conductivity ratio of Al<sub>2</sub>O<sub>3</sub>/EG nanofluid by applying least squares support vector machine (LSSVM) and genetic algorithm as a connectionist approach. *Journal of Thermal Analysis and Calorimetry*, 1–11.

[Web of Science ®](#) | [Google Scholar](#)

3. Ahmadi, M. H., Mahian, O., Nazari, M. A., & Ghasempour, R. (2018). A review of thermophysical properties of nanofluids. *Journal of Thermal Analysis and Calorimetry*, 188, 188–198.

4. Ahmadi, M. H., Mahian, O., Nazari, M. A., & Ghasempour, R. (2018). A review of thermophysical properties of nanofluids. *Journal of Thermal Analysis and Calorimetry*, 188, 188–198.

### About Cookies On This Site

We and our partners use cookies to enhance your website experience, learn how our site is used, offer personalised features, measure the effectiveness of our services, and tailor content and ads to your interests while you navigate on the web or interact with us across devices. You can choose to accept all of these cookies or only essential cookies. To learn more or manage your preferences, click “Settings”. For further information about the data we collect from you, please see our [Privacy Policy](#).

Accept All

Essential Only

Settings



5. Ahmadi, M. H., Tatar, A., Seifaddini, P., Ghazvini, M., Ghasempour, R., & Sheremet, M. A. (2018). Thermal conductivity and dynamic viscosity modeling of Fe<sub>2</sub>O<sub>3</sub>/water nanofluid by applying various connectionist approaches. *Numerical Heat Transfer, Part A: Applications*, 74, 1–22.

 | [Web of Science®](#) | [Google Scholar](#)

6. Alade, I. O., Oyehan, T. A., Popoola, I. K., Olatunji, S. O., & Bagudu, A. (2018). Modeling thermal conductivity enhancement of metal and metallic oxide nanofluids using support vector regression. *Advanced Powder Technology*, 29(1), 157–167.

 | [Web of Science®](#) | [Google Scholar](#)

7. Asadi, M., & Asadi, A. (2016). Dynamic viscosity of MWCNT/ZnO-engine oil hybrid nanofluid: An experimental investigation and new correlation in different temperatures and solid concentrations. *International Communications in Heat and Mass Transfer*, 76, 41–45.

 | [Web of Science®](#) | [Google Scholar](#)

8. Baghban, A., Jalali, A., Shafiee, M., Ahmadi, M. H., & Chau, K.-W. (2019). Developing an ANFIS-based swarm concept model for estimating the relative viscosity of nanofluids. *Engineering Applications of Computational Fluid Mechanics*, 13(1), 26–39.

 | [Web of Science®](#) | [Google Scholar](#)

9. Baghban, A., Kahani, M., Nazari, M. A., Ahmadi, M. H., & Yan, W.-M. (2019). Sensitivity analysis and application of machine learning methods to predict the heat transfer performance of CNT/water nanofluid flow through coils. *International Journal of Heat and Mass Transfer*.

### About Cookies On This Site

We and our partners use cookies to enhance your website experience, learn how our site is used, offer personalised features, measure the effectiveness of our services, and tailor content and ads to your interests while you navigate on the web or interact with us across devices. You can choose to accept all of these cookies or only essential cookies. To learn more or manage your preferences, click “Settings”. For further information about the data we collect from you, please see our [Privacy Policy](#).

 Accept All



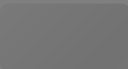
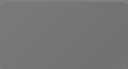

Essential Only


Settings



10. Baghban, A., Kahani, M., Nazari, M. A., Ahmadi, M. H., & Yan, W.-M. (2019). Sensitivity analysis and application of machine learning methods to predict the heat transfer performance of CNT/water nanofluid flow through coils. *International Journal of Heat and Mass Transfer*.



1. Chau, K.-W. (2017). Use of meta-heuristic techniques in rainfall-runoff modelling. Multidisciplinary Digital Publishing Institute, 186.  
 | [Web of Science ®](#) | [Google Scholar](#)
2. Chiam, H., Azmi, W., Usri, N., Mamat, R., & Adam, N. (2017). Thermal conductivity and viscosity of Al<sub>2</sub>O<sub>3</sub> nanofluids for different based ratio of water and ethylene glycol mixture. Experimental Thermal and Fluid Science, 81, 420–429.  
 | [Web of Science ®](#) | [Google Scholar](#)
3. Chou, S.-M., Lee, T.-S., Shao, Y. E., & Chen, I.-F. (2004). Mining the breast cancer pattern using artificial neural networks and multivariate adaptive regression splines. Expert Systems with Applications, 27(1), 133–142.  
 | [Web of Science ®](#) | [Google Scholar](#)
4. De Cos Juez, F. J., Lasheras, F. S., García Nieto, P. J., & Suárez, M. S. (2009). A new data mining methodology applied to the modelling of the influence of diet and lifestyle on the value of bone mineral density in post-menopausal women. International Journal of Computer Mathematics, 86(10-11), 1878–1887.  
 | [Web of Science ®](#) | [Google Scholar](#)
5. Ebrahimi-Moghadam, A., Mohseni-Gharyehsafa, B., & Farzaneh-Gord, M. (2018). Using artificial neural network and quadratic algorithm for minimizing entropy generation of Al<sub>2</sub>O<sub>3</sub>-EG/W nanofluid flow inside parabolic trough solar collector. Renewable Energy, 129, 473–485.  
 | [Web of Science ®](#) | [Google Scholar](#)

6. Esfe, M. H., Saedodin, S., Bighari, M., & Rostamian, H. (2016). An experimental study on the effect of nanoparticle concentration on the thermal conductivity of water. International Journal of Heat and Mass Transfer, 59(1), 1–11.  
 | [Web of Science ®](#) | [Google Scholar](#)
7. Friedmann, J. (2017). Statistical analysis of the data collected from the study of the effect of the use of the mobile phone on the health of the population. In this article

#### About Cookies On This Site

We and our partners use cookies to enhance your website experience, learn how our site is used, offer personalised features, measure the effectiveness of our services, and tailor content and ads to your interests while you navigate on the web or interact with us across devices. You can choose to accept all of these cookies or only essential cookies. To learn more or manage your preferences, click “Settings”. For further information about the data we collect from you, please see our [Privacy Policy](#).

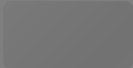

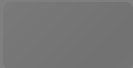

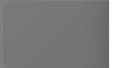
Accept All

Essential Only

Settings





8. Friedman, J. H., & Roosen, C. B. (1995). An introduction to multivariate adaptive regression splines. *Statistical Methods in Medical Research*, 4, 197–217.  
 | [PubMed](#) | [Google Scholar](#)
9. Gardner, M. W., & Dorling, S. (1998). Artificial neural networks (the multilayer perceptron)—a review of applications in the atmospheric sciences. *Atmospheric Environment*, 32(14-15), 2627–2636.  
 | [Web of Science ®](#) | [Google Scholar](#)
10. Goda, H. M., Shokir, E.-M., Eissa, M., Fattah, K. A., & Sayyoun, M. H. (2003). Prediction of the PVT data using neural network computing theory. *Nigeria annual international conference and exhibition*.  
[Google Scholar](#)
11. Hajikhodaverdikhan, P., Nazari, M., Mohsenizadeh, M., Shamshirband, S., & Chau, K.-W. (2018). Earthquake prediction with meteorological data by particle filter-based support vector regression. *Engineering Applications of Computational Fluid Mechanics*, 12(1), 679–688.  
 | [Web of Science ®](#) | [Google Scholar](#)
12. Hornik, K., Stinchcombe, M., & White, H. (1989). Multilayer feedforward networks are universal approximators. *Neural Networks*, 2(5), 359–366.  
 | [Web of Science ®](#) | [Google Scholar](#)
13. Hosseini, F., Kasaeian, A., Pourfayaz, F., Sheikhpour, M., & Wen, D. (2018). Novel ZnO-Ag/MWCNT nanocomposite for the photocatalytic degradation of phenol. *Materials Science in Semiconductor Processing*, 83, 175–185.  


#### About Cookies On This Site

We and our partners use cookies to enhance your website experience, learn how our site is used, offer personalised features, measure the effectiveness of our services, and tailor content and ads to your interests while you navigate on the web or interact with us across devices. You can choose to accept all of these cookies or only essential cookies. To learn more or manage your preferences, click “Settings”. For further information about the data we collect from you, please see our [Privacy Policy](#).

 Accept All

Essential Only

Settings

14. Kazem, K., & Chau, K.-W. (2018). Machine learning for fluid



25. Mohseni-Gharyehsafa, B., Ebrahimi-Moghadam, A., Okati, V., Farzaneh-Gord, M., Ahmadi, M. H., & Lorenzini, G. (2018). Optimizing flow properties of the different nanofluids inside a circular tube by using entropy generation minimization approach. *Journal of Thermal Analysis and Calorimetry*, 1–11.

 | [Web of Science ®](#) | [Google Scholar](#)

26. Nazari, M. A., Ahmadi, M. H., Ghasempour, R., & Shafii, M. B. (2018). How to improve the thermal performance of pulsating heat pipes: A review on working fluid. *Renewable and Sustainable Energy Reviews*, 91, 630–638.

 | [Web of Science ®](#) | [Google Scholar](#)

27. Nazari, M. A., Ghasempour, R., Ahmadi, M. H., Heydarian, G., & Shafii, M. B. (2018). Experimental investigation of graphene oxide nanofluid on heat transfer enhancement of pulsating heat pipe. *International Communications in Heat and Mass Transfer*, 91, 90–94.

 | [Web of Science ®](#) | [Google Scholar](#)

28. Nieto, P. G., & Antón, J.Á. (2014). Nonlinear air quality modeling using multivariate adaptive regression splines in Gijón urban area (Northern Spain) at local scale. *Applied Mathematics and Computation*, 235, 50–65.

 | [Web of Science ®](#) | [Google Scholar](#)

29. Nieto, P. G., Fernández, J. A., Lasheras, F. S., de Cos Juez, F., & Muñiz, C. D. (2012). A new improved study of cyanotoxins presence from experimental cyanobacteria concentrations in the Trasona reservoir (Northern Spain) using the MARS technique. *Science of the Total Environment*, 430, 88–92.

 | [PubMed](#) | [Web of Science ®](#) | [Google Scholar](#)

### About Cookies On This Site

We and our partners use cookies to enhance your website experience, learn how our site is used, offer personalised features, measure the effectiveness of our services, and tailor content and ads to your interests while you navigate on the web or interact with us across devices. You can choose to accept all of these cookies or only essential cookies. To learn more or manage your preferences, click “Settings”. For further information about the data we collect from you, please see our [Privacy Policy](#).

 Accept All





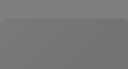
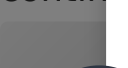
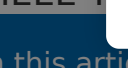
Essential Only

Settings

30. Nieto, P. G., & Antón, J.Á. (2016). Nonlinear air quality modeling using multivariate adaptive regression splines in Gijón urban area (Northern Spain) at local scale. *Applied Mathematics and Computation*, 298, 1–11.

[Web of Science](#)



1. Nieto, P. G., Lasheras, F. S., de Cos Juez, F., & Fernández, J. A. (2011). Study of cyanotoxins presence from experimental cyanobacteria concentrations using a new data mining methodology based on multivariate adaptive regression splines in Trasona reservoir (Northern Spain). *Journal of Hazardous Materials*, 195, 414-421.  
 | [PubMed](#) | [Web of Science ®](#) | [Google Scholar](#)
2. Nikkam, N., & Toprak, M. S. (2018). Fabrication and thermo-physical characterization of silver nanofluids: An experimental investigation on the effect of base liquid. *International Communications in Heat and Mass Transfer*, 91, 196-200.  
 | [Web of Science ®](#) | [Google Scholar](#)
3. Orhan, U., Hekim, M., & Ozer, M. (2011). EEG signals classification using the K-means clustering and a multilayer perceptron neural network model. *Expert Systems with Applications*, 38(10), 13475-13481.  
 | [Web of Science ®](#) | [Google Scholar](#)
4. Ramezanizadeh, M., Alhuyi Nazari, M., Ahmadi, M. H., & Chau, K.-W. (2019). Experimental and numerical analysis of a nanofluidic thermosyphon heat exchanger. *Engineering Applications of Computational Fluid Mechanics*, 13(1), 40-47.  
 | [Web of Science ®](#) | [Google Scholar](#)
5. Rezaei, M. H., Sadeghzadeh, M., Alhuyi Nazari, M., Ahmadi, M. H., & Astaraei, F. R. (2018). Applying GMDH artificial neural network in modeling CO2 emissions in four nordic countries. *International Journal of Low-Carbon Technologies*, 13(3), 266-271.  
 | [Web of Science ®](#) | [Google Scholar](#)
6. Royston, P., & Sauerbrei, W. (2008). Multivariable model building: A pragmatic approach to continuous variables. *Statistical Modelling*, 8(2), 401-414.  
 | [Web of Science ®](#) | [Google Scholar](#)
7. Ruck, L. T., & Sauerbrei, W. (2008). Multivariable model building: A pragmatic approach to continuous variables. *Statistical Modelling*, 8(2), 401-414.  
 | [Web of Science ®](#) | [Google Scholar](#)

### About Cookies On This Site

We and our partners use cookies to enhance your website experience, learn how our site is used, offer personalised features, measure the effectiveness of our services, and tailor content and ads to your interests while you navigate on the web or interact with us across devices. You can choose to accept all of these cookies or only essential cookies. To learn more or manage your preferences, click "Settings". For further information about the data we collect from you, please see our [Privacy Policy](#).

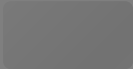
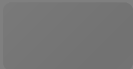
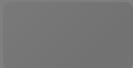
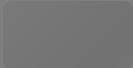


Accept All

Essential Only

Settings





38. Saidur, R., Leong, K., & Mohammad, H. (2011). A review on applications and challenges of nanofluids. *Renewable and Sustainable Energy Reviews*, 15(3), 1646–1668.
-  | [Web of Science ®](#) | [Google Scholar](#)
39. Sinha, P. (2013). Multivariate polynomial regression in data mining: Methodology, problems and solutions. *International Journal of Scientific and Engineering Research*, 4(12), 962–965.
- [Google Scholar](#)
40. Soltani, O., & Akbari, M. (2016). Effects of temperature and particles concentration on the dynamic viscosity of MgO-MWCNT/ethylene glycol hybrid nanofluid: Experimental study. *Physica E: Low-Dimensional Systems and Nanostructures*, 84, 564–570.
-  | [Web of Science ®](#) | [Google Scholar](#)
41. Taormina, R., Chau, K.-W., & Sivakumar, B. (2015). Neural network river forecasting through baseflow separation and binary-coded swarm optimization. *Journal of Hydrology*, 529, 1788–1797.
-  | [Web of Science ®](#) | [Google Scholar](#)
42. Vanzella, E., Cristiani, S., Fontana, A., Nonino, M., Arnouts, S., Giallongo, E., ... Zaggia, S. (2004). Photometric redshifts with the multilayer perceptron neural network: Application to the HDF-S and SDSS. *Astronomy & Astrophysics*, 423(2), 761–776.
-  | [Web of Science ®](#) | [Google Scholar](#)
43. Vasanthakumari, R., & Pondy, P. (2018). Mixed convection of silver and titanium dioxide nanofluids along inclined stretching sheet in presence of MHD with heat generation. *Journal of Heat and Mass Transfer*, 5(2), 123–134.
-  | [Web of Science ®](#) | [Google Scholar](#)
44. Wang, Y., & Zhang, X. (2019). Numerical simulation of heat pipe performance in microgravity. *International Journal of Heat and Mass Transfer*, 62(1), 1–15.
-  | [Web of Science ®](#) | [Google Scholar](#)

#### About Cookies On This Site

We and our partners use cookies to enhance your website experience, learn how our site is used, offer personalised features, measure the effectiveness of our services, and tailor content and ads to your interests while you navigate on the web or interact with us across devices. You can choose to accept all of these cookies or only essential cookies. To learn more or manage your preferences, click “Settings”. For further information about the data we collect from you, please see our [Privacy Policy](#).




Accept All

Essential Only

Settings





5. Wu, C., & Chau, K. (2011). Rainfall-runoff modeling using artificial neural network coupled with singular spectrum analysis. *Journal of Hydrology*, 399(3-4), 394-409.
-  | [Web of Science ®](#) | [Google Scholar](#)
16. Xu, Q.-S., Daszykowski, M., Walczak, B., Daeyaert, F., De Jonge, M., Heeres, J., ... Massart, D. L. (2004). Multivariate adaptive regression splines—studies of HIV reverse transcriptase inhibitors. *Chemometrics and Intelligent Laboratory Systems*, 72(1), 27-34.
-  | [Web of Science ®](#) | [Google Scholar](#)
17. Zeinali Heris, S., Kazemi-Beydokhti, A., Noie, S., & Rezvan, S. (2012). Numerical study on convective heat transfer of Al<sub>2</sub>O<sub>3</sub>/water, CuO/water and Cu/water nanofluids through square cross-section duct in laminar flow. *Engineering Applications of Computational Fluid Mechanics*, 6(1), 1-14.
-  | [Web of Science ®](#) | [Google Scholar](#)

[Download PDF](#)

## Related research

People also read

Recommended articles

Cited by  
35



### About Cookies On This Site

We and our partners use cookies to enhance your website experience, learn how our site is used, offer personalised features, measure the effectiveness of our services, and tailor content and ads to your interests while you navigate on the web or interact with us across devices. You can choose to accept all of these cookies or only essential cookies. To learn more or manage your preferences, click "Settings". For further information about the data we collect from you, please see our [Privacy Policy](#).

 Accept All

Essential Only

Settings



## Information for

Authors

R&D professionals

Editors

Librarians

Societies

## Opportunities

Reprints and e-prints

Advertising solutions

Accelerated publication

Corporate access solutions

## Open access

Overview

Open journals

Open Select

Dove Medical Press

F1000Research

## Help and information

Help and contact

Newsroom

All journals

Books

## Keep up to date

Register to receive personalised research and resources by email

 Sign me up



Copyright © 2024 Informa UK Limited [Privacy policy](#) [Cookies](#) [Terms & conditions](#)

[Accessibility](#)

 Taylor & Francis Group  
an informa business

Registered in England & Wales No. 3099067  
5 Howick Place | London | SW1P 1WG

### About Cookies On This Site

We and our partners use cookies to enhance your website experience, learn how our site is used, offer personalised features, measure the effectiveness of our services, and tailor content and ads to your interests while you navigate on the web or interact with us across devices. You can choose to accept all of these cookies or only essential cookies. To learn more or manage your preferences, click “Settings”. For further information about the data we collect from you, please see our [Privacy Policy](#).

 Accept All

Essential Only

Settings

In this article

